J|A|C|S
ARTICLES
Published on Web 12/08/2006

Self-Organization of Polybases Neutralized with Mesogenic Wedge-Shaped Sulfonic Acid Molecules: An Approach toward Supramolecular Cylinders

Xiaomin Zhu,[†] Uwe Beginn,*[,†] Martin Möller,*[,†] Raluca I. Gearba,[‡] Denis V. Anokhin,[‡] and Dimitri A. Ivanov[‡,§]

Contribution from the DWI an der RWTH Aachen e.V. and Institute of Technical and Macromolecular Chemistry at RWTH Aachen, Pauwelsstrasse 8, D-52056 Aachen, Germany, Institut de Chimie des Surfaces et Interfaces, 15 rue Jean Starcky, 68057 Mulhouse Cedex, France, and Laboratoire de Physique des Polymères, CP 223, Université Libre de Bruxelles, Boulevard du Triomphe, B-1050 Brussels, Belgium

Received August 17, 2006; E-mail: beginn@dwi.rwth-aachen.de; moeller@dwi.rwth-aachen.de

Abstract: Complexes consisting of poly(4-vinylpyridine) and mesogenic wedge-shaped ligands 4′-[3″,4″,5″-tris(dodecyloxy)benzoyloxy]azobenzene-4-sulfonic acid and 4′-[3″,4″,5″-tris(octyloxy)benzoyloxy]azobenzene-4-sulfonic acid have been prepared with different monomer/ligand ratios. Upon protonation of the poly(4-vinylpyridine) chains by the wedge-shaped sulfonic acid molecules a hypsochromic and hyperchromic effect was observed with the $\pi-\pi^*$ transition of the azo-chromophor, allowing us to monitor the neutralization process by means of UV−vis spectroscopy in solution. The changes of the absorption characteristics implied a conformational change of the polymer backbone. In the bulk the interaction between pyridine and sulfonic acid moieties was proved by FT-IR spectroscopy. Polarizing optical microscopy, differential scanning calorimetry, and X-ray diffraction measurements were used to study the bulk structure of the complexes. The complexes formed a liquid crystalline lamellar phase at low degrees of substitution, while a hexagonal columnar mesophase was observed at degrees of neutralization of 80% and higher.

Introduction

Supramolecular self-organization is a powerful tool for producing functional materials.[1] During the past decade a concept based on complexation of polymer chains by low molecular weight amphiphiles via noncovalent interactions such as ionic interaction, coordination interaction, or hydrogen bonding has become a common tool in the construction of nanostructured macromolecular materials.[2] The polymer chains and low molecular weight ligands combine to form comb-shaped supramolecules ("complexes"), which in turn self-assemble on a length scale of a few nanometers. Due to the incompatibility between the polymer and the nonpolar part of the ligand molecules, these complexes form microphase-separated morphologies. Most frequently lamellar phases are obtained, where layers of ligands and layers of polymers alternate.[3]

On the other hand, it is well-established that wedge-shaped amphiphilic molecules with a polar head at the tip of the wedge and a large nonpolar body can self-assemble into well-defined cylindrical structures.[4] Macromolecules bearing wedge-shaped side groups covalently attached to the polymer backbone have also been synthesized and studied.[5] Such monodendron-jacketed polymers were shown to form columnar structures, and it was also found that the self-assembly of the monodendron-side groups to a cylindrical structure could induce the formation of a disordered helical conformation of the polymer backbone.[6]

It has been reported that the complexation of polybases with low molecular weight sulfonic acids transforms insoluble macromolecules like polyaniline into soluble materials;[7] however, the obtained complexes mainly did not exhibit columnar superstructures. Recently our group have developed a new class

[†] DWI an der RWTH Aachen e.V. and Institute of Technical and Macromolecular Chemistry at RWTH Aachen.
[‡] Institut de Chimie des Surfaces et Interfaces.
[§] Université Libre de Bruxelles.

(1) Lehn, J.-M. *Supramolecular Chemistry. Concepts and perspectives*; VCH: Weinheim, Germany, 1995.
(2) (a) Antonietti, M.; Thünemann, A. *Curr. Opin. Colloid Interface Sci.* **1996**, *1*, 667−671. (b) Ikkala, O.; ten Brinke, G. *Science* **2002**, *295*, 2407−2409. (c) Pollino, J. M.; Weck, M. *Chem. Soc. Rev.* **2005**, *34*, 193−207. (d) MacKnight, W. J.; Ponomarenko, E. A.; Tirrell, D. A. *Acc. Chem. Res.* **1998**, *31*, 781−788. (e) Zhou, S.; Chu, B. *Adv. Mater.* **2000**, *12*, 545−556.
(3) (a) Antonietti, M.; Conrad, J.; Thünemann, A. *Macromolecules* **1994**, *27*, 6007−6011. (b) Ikkala, O.; Ruokolainen, J.; ten Brinke, G.; Torkkeli, M.; Mäkelä, T.; Serimaa, R. *Macromolecules* **1995**, *28*, 7088−7094. (c) Ruokolainen, J.; ten Brinke, G.; Ikkala, O.; Torkkeli, M.; Serimaa, R. *Macromolecules* **1996**, *29*, 3409−3415. (d) Bazuin, C. G; Brodin, C. *Macromolecules* **2004**, *37*, 9366−9372. (e) Ujiie, S.; Takagi, S.; Sato, M. *High Perform. Polym.* **1998**, *10*, 139−146. (f) Tal'roze, R. V.; Kuptsov, S. A.; Sycheva, T. I.; Bezborodov, V. S.; Plate, N. A. *Macromolecules* **1996**, *28*, 8689−8691.
(4) (a) Beginn, U.; *Prog. Polym. Sci.* **2003**, *28*, 1049−1105. (b) Beginn, U.; Lattermann, G. *Mol. Cryst. Liq. Cryst.* **1994**, *241*, 215−219. (c) Percec, V.; Heck, J.; Johansson, G.; Tomazos, D.; Ungar, G. *Macromol. Symp.* **1994**, *77*, 237−265.
(5) Percec, V.; Ahn, C.-H.; Ungar, G.; Yeardley, D. J. P.; Möller, M.; Sheiko, S. *Nature (London)* **1998**, *391*, 161−164.
(6) (a) Kwon, Y. K.; Chvalun, S.; Scheider, A.-I.; Blackwell, S.; Percec, V.; Heck, J. A. *Macromolecules* **1994**, *27*, 6129−6132. (b) Prokhorova, S. A.; Sheiko, S. S.; Möller, M.; Ahn, C.-H.; Percec, V. *Macromol. Rapid Commun.* **1998**, *19*, 359−366.
(7) Cao, Y.; Smith, P. *Polymer* **1983**, *34*, 3139−3143.

10.1021/ja065968v CCC: $33.50

of self-assembling wedge-shaped amphiphiles that bear a sulfonic acid group at the tip of the wedge, being able to form thermotropic columnar mesophases in the bulk and discrete cylindrical superstructures from dilute solution.[8] In this work we combine the structuring abilities of wedge-shaped sulfonic acids and the ligand acid/polybase complexation concept to generate a new class of macromolecular material. Poly(vinylpyridines) are neutralized with wedge-shaped sulfonic acids to produce supramolecular cylinders. Since the neutralization enthalpy of polyvinylpyridine units with sulfonic acids ($\sim$60−75 kJ mol^{-1}/monomer unit)[9] by far exceeds the entropy contribution of chain stretching ($T\Delta S_{\text{stretch}} \approx 1.25$ kJ mol^{-1}/monomer unit at 300 K),[10] the formation of elongated cylindrical structures containing at least partially stretched polymer chains in their interior is a thermodynamically allowed process.

In contrast to comblike molecules with flexible linear side chains, the formation of a cylindrical structure will be predominately driven by self-assembly of the side groups, and not by the entropic repulsion/excluded volume effects of the side chains.[11] Thus, in this way one can mimic the architecture of the tobacco mosaic virus, in which a helical RNA chain is complexed by self-assembled identical protein molecules via noncovalent weak interactions.[12] In this structure the length of the virus is controlled by the length of the central RNA macromolecule. In our case the natural protein building blocks are replaced by low molecular weight wedge-shaped molecules, and the RNA is represented by a synthetic macromolecular chain. As a model system we have chosen poly(4-vinylpyridine) (P4VP) as the synthetic polymer chain bearing basic pyridine groups, which can be protonated by sulfonic acid molecules.

Scheme 1. Preparation of **P4VP(C*m*-H)$_{DN}$** Complexes of Poly(4-vinylpyridine) (P4VP) with Wedge-Shaped Sulfonic Acid Molecules **C*m*-H** (m = 8, 12)[a]

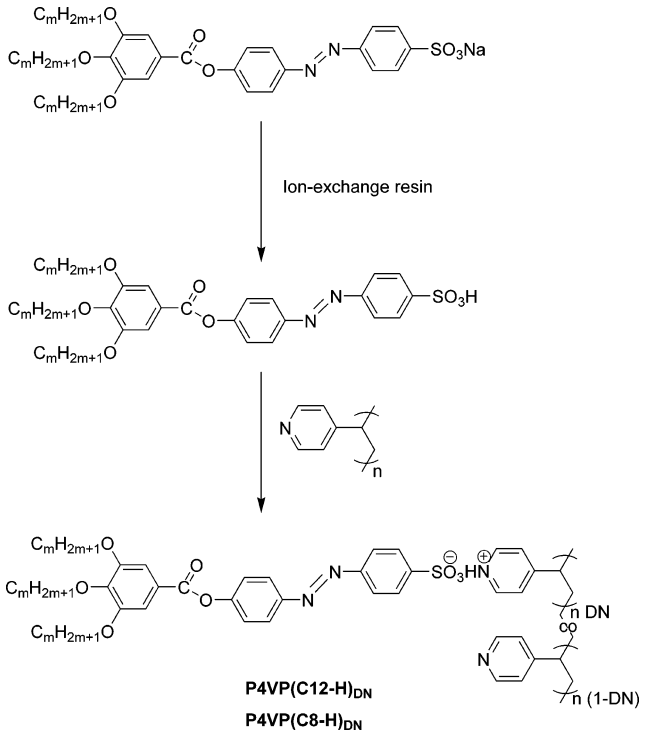

[a] Key: DN, degree of neutralization; **C*m*-X**, wedge-shaped sulfonate amphiphiles (m = 8, 12, X = H, Na, Py (pyridinium)).

Experimental Details

Materials. The synthesis of sodium and pyridinium 4′-[3″,4″,5″-tris(dodecyloxy)benzoyloxy]azobenzene-4-sulfonate (**C12-Na**) and 4′-[3″,4″,5″-tris(octyloxy)benzoyloxy]azobenzene-4-sulfonate (**C8-Na**) was described elsewhere.[8] The purity of the compounds exceeded 98% as tested by TLC, ^{1}H NMR, and elemental analysis.

Amberlyst 15 ion-exchange resin (Aldrich), diisopropyl ether (pa, Merck), chloroform (pa, Merck), and isobutyl acetate (puriss, Fluka) were used as received. For UV−vis spectroscopy chloroform for the spectroscopy (Uvasol, Merck) was used. Poly(4-vinylpyridine) (P4VP) (M_n = 46 700, M_w = 53 200) was purchased from Polymer Source Inc. It was dried in vacuum at 60 °C for 36 h prior to use.

Preparation of Polymer−Sulfonic Acid Complexes. The synthesis of polymer−sulfonic acid complexes is outlined in Scheme 1. A solution of 100.0 mg (0.104 mmol) of sodium sulfonate (**C12-Na**) in 10 mL of diisopropyl ether was shaken over night with 1 g of Amberlyst 15 ion-exchange resin. The resulting solution was filtered through a glass filter (pore size 4), and the ion-exchange resin was washed with diisopropyl ether until a colorless filtrate was obtained. The combined filtrates were added to a well-stirred solution of 11.0 mg (0.104 mmol of pyridine units) of P4VP in chloroform (concentration of P4VP was always 1.0 mg/mL) to prepare the complex with full neutralized pyridine units. The resulting solution was stirred for additional 2 h. Subsequently the solvent was removed under reduced pressure on a rotor evaporator. The product was dried in vacuum at 40 °C for 6 h. The complexes with C8-H were synthesized according to the same procedure. The complexes are denoted as **P4VP(C12-H)$_{DN}$** and **P4VP(C8-H)$_{DN}$**, where DN is the degree of neutralization. The yields were 96−98%. The compositions and yields of the different reaction mixtures can be found in the Supporting Information.

Techniques. Infrared spectra (IR) were recorded with a Nicolet 710 FT-IR spectrometer using a photoacoustic technique. The measurements were performed with a few milligrams of sample placed in a small aluminum pan.

For thermo−optical analysis a Carl Zeiss Axioplan 2 imaging polarizing microscope equipped with a Mettler Toledo FP 82HT hot stage connected to a Mettler Toledo FP 90 processor was used. The micrographs recorded with a Carl Zeiss AxioCam MRc digital camera.

Differential scanning calorimetry (DSC) measurements were performed using a Netzsch DSC 204 unit. Samples (typical weight: 5 mg) were enclosed in standard Netzsch 25 μL aluminum crucibles. Indium and palmitic acid were used as temperature calibration standards. The employed heating and cooling rates were 10 K min^{-1}. For quenching a cooling rate of 40 K min^{-1} was used.

UV−vis spectra were recorded in chloroform solution at room temperature on a Perkin-Elmer Lambda EZ210 UV−vis spectrometer at a scan rate of 100 nm min^{-1}. The slit width was 2 nm. Three concentrations (c < 0.08 mg/mL) were prepared to determine the molar extinction coefficient ϵ_{328} of the wedge-shaped sulfonic acid using Beer's law according to the following:

$$\epsilon_{328} = A_{328}/(c_M L) \quad (1)$$

$$c_M = c/(M_{\text{sulfonic acid}} + M_{4VP}/\text{DN}) \quad (2)$$

Here ϵ_{328} = molar extinction coefficient at a wavelength of 328 nm, A_{328} = absorbance at 328 nm, c_M = molar concentration of the wedge-

(8) Zhu, X.; Tartsch, B.; Beginn, U.; Möller, M. *Chem.—Eur. J.* **2004**, *10*, 3871−3878.
(9) Arnett, E. A.; Ahsan, T.; Amarnath, K. *J. Am. Chem. Soc.* **1991**, *113*, 6858−6861.
(10) Vollmert, B. *Grundriss der Makromolekularen Chemie*; E. Vollmert Verlag: Karlsruhe, Germany, 1985.
(11) Frederickson, G. H. *Macromolecules* **1993**, *26*, 2825−2831.
(12) (a) Klug, A. *Angew. Chem.* **1983**, *95*, 579−96. (b) Klug, A. *Philos. Trans. R. Soc. London, Ser .B* **1999**, *354*, 531−535. (c) Martin, S. J. *The biochemistry of viruses*; Cambridge University Press: London, New York, Melbourne, 1978.

Table 1. Thermal Transitions of the Wedge-Shaped Sulfonates Determined during Heating by DSC and POM

compd	phase type, transition temps, °C (enthalpies, kJ mol^{-1})
C8-Na	Lam,[a] 84 °C (25.0); Col_{hd},[b] 300 °C I[c]
C8-Py	Lam, 109 °C (25.2); Col_{hd},210 °C I
C12-Na	Lam, ~50 °C; Col_{hd}, >300 °C I
C12-Py	Lam, 94 °C (63.5); Col_{hd}, 200 °C I

[a] Lam = lamellar phase. [b] Col_{hd} = disordered columnar hexagonal phase. [c] Isotropization temperatures were measured by POM and were accompanied by decomposition. [d] The data for **C12-Na** and **C12-Py** are taken from the literature.[8]

shaped sulfonic acid in solution, L = optical path length = 1 cm, c = concentration of complexes in solution in g/L, $M_{\text{sulfonic acid}}$ and M_{4VP} = molar mass of wedge-shaped sulfonic acids and 4-vinylpyridine monomer unit, respectively, and DN = degree of neutralization.

^{1}H NMR spectra were recorded with a Varian VXR 300 instrument at 300 MHz using TMS as internal standard. $CDCl_3$ was used as solvent. The concentration of the solution was 15−30 mg/mL.

X-ray diffraction experiments were performed on the ID2 and BM26 beamlines at the European Synchrotron Radiation Facility, ESRF (Grenoble, France). The energy of the X-ray photons was 10 keV. The diffraction patterns were collected on powders as well as on oriented samples in transmission. The s-axis ($s = 2\sin(\theta)/\lambda$, where θ is the Bragg angle and λ is the wavelength) was calibrated using several diffraction orders of silver behenate. Oriented samples of **P4VP(C12-H)$_{DN}$** complexes were prepared by swelling in isobutyl acetate and subsequent extrusion using a home-built miniextruder. The resulting fiber samples (0.7 mm in diameter) were subsequently dried at 60 °C for 2 h. The 2D X-ray patterns patterns were collected using X-ray sensitive Fuji image plates, which were scanned with a pixel size of 200 × 200 μm^2. X-ray patterns of **P4VP(C8-H)$_{DN}$** complexes were recorded on powder samples. Temperature dependence of the interlayer distance was studied from 25 to 160 °C at a heating rate of 10 K min^{-1}. One pattern was recorded every 2.5 °C using a CCD camera.

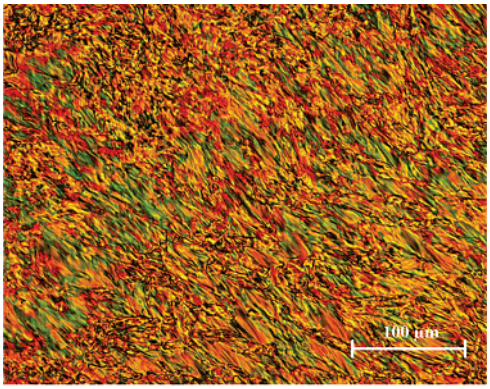

(a)

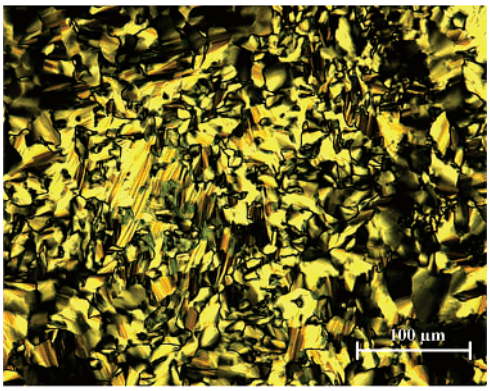

(b)

Figure 1. Polarizing optical micrographs of **C8-Py** (a) and **C8-Na** (b) at 200 °C.

Results and Discussion

The chemical structures of the wedge-shaped sulfonic acid molecules used as ligands to complex poly(4-vinylpyridine) (P4VP), namely 4′-[3″,4″,5″-tris(dodecyloxy)benzoyloxy]-azobenzene-4-sulfonic acid (**C12-H**) and 4′-[3″,4″,5″-tris-(octyloxy)benzoyloxy]azobenzene-4-sulfonic acid (**C8-H**) are depicted in Scheme 1. The wedge-shaped sulfonic acid molecules **C8-H** and **C12-H** were synthesized according to the literature.[8] The azo-chromophore was deliberately incorporated as a probe to follow the self-assembling process by monitoring changes in the spectral properties of the respective $\pi-\pi^*$ transition. Furthermore, cis−trans photoisomerization of the azo-moiety will alter the molecular geometry of the ligand and may change its self-organization properties.

The sodium sulfonate salts **C*m*-Na** could easily be converted in diisopropyl ether by ion exchange to the corresponding sulfonic acids (cf. Scheme 1) that are stable in diluted solution.[8] It has been suggested in the literature that the homogeneous protonation of poly(vinylpyridine) takes place only at low concentrations of acid and polybase.[3b] By the mixing of the acid solutions with corresponding amounts of poly(4-vinylpyridine) dissolved in chloroform (cf. experimental part), the macromolecular **P4VP(C*m*-H)$_{DN}$** ($0 \le$ **DN** $\le$ **1**) complexes are obtained. Here "DN" denotes the theoretical degree of neutralization, i.e., the molar fraction of present vinylpyridine monomer units that can become protonated by the added amount of ligand acid molecules. Complexes with high DN values, such as **P4VP-(C12-H)$_{1.0}$**, **P4VP(C12-H)$_{0.8}$**, and **P4VP(C8-H)$_{1.0}$**, were obtained in form of dark brown powders, while the other complexes were orange.

Prior to the macromolecular complexes the phase transitions of the sodium (**C8-Na**, **C12-Na**) and pyridinium (**C8-Py**, **C12-Py**) sulfonate ligands were characterized by DSC, POM, and X-ray diffraction. The characteristic temperatures of these compounds are summarized in Table 1.

The clearing temperatures of the pyridinium derivatives are between 200 °C (**C12-Py**) and 210 °C (**C8-Py**), while the sodium salts become isotropic above 300 °C. DSC revealed a first-order phase transition upon heating of all the studied compounds. It is worth noting that the reverse process on cooling is very slow in the bulk. POM observations show that the high-temperature phases of **C8-Py** and **C8-Na** exhibit fan-shaped textures (Figure 1), which may indicate the presence of a lamellar or a disordered columnar hexagonal (Col_{hd}) phase. A miscibility experiment has been carried out in the low and high temperature mesophases of **C12-Py** with **C8-Py**. It has been found that both compounds were completely miscible in the respective phases. According to the Arnold−Sackmann rule **C12-Py** and **C8-Py** should hence form the same phase sequence. The supramolecular organization of the wedge-shaped sulfonates has been studied by X-ray diffraction experiments. The detailed data analysis is given in Supporting Information. To summarize, all the sulfonate amphiphiles tend to form lamellar phases at low temperatures, which transform into a Col_{hd} phase upon heating. The pyridinium salts exhibit slightly larger lattice parameter as compared to the sodium salts.

Table 2. Comparison of the Solubility of **P4VP(C12-H)$_{DN}$** Complexes with P4VP (2 mg of Compound in 1 mL of Solution)

		complexes		
solvent	P4VP	DN[a] = 0.25	DN = 0.50	DN = 1.0
ethanol	yes	no	no	no
dimethylformamide	yes	yes	no	no
chloroform	yes	yes	yes	yes
tetrahydrofuran	no	yes	yes	yes
toluene	no	yes	yes	yes
n-hexane	no	no	partially soluble	yes

[a] DN = degree of neutralization.

As depicted in Scheme 1, the sodium salts were used to prepare the corresponding sulfonic acids that were subsequently added to poly(4-vinylpyridine) solutions. Hence, the pyridinium salts **C8-Py** and **C12-Py** can be regarded as model compounds, i.e., the monomeric analogs of the macromolecular complexes with DN = 1.0. With the macromolecular complexes the degree of substitution was varied from 0.13 to 1.0 to study the structural properties with increasing space-filling around the polymer backbones.

The first indication of the complex formation is the change in solubility of the complexes in comparison to pure P4VP (Table 2). P4VP is a polar polymer soluble in (semi)polar solvents like ethanol, dimethylformamide (DMF), and chloroform. Neutralization of P4VP by wedge-shaped sulfonic molecules with bulky nonpolar alkyl chains leads to the inversion of the polarity, since the complexes become insoluble in polar solvents like ethanol and DMF but are well-soluble in nonpolar solvents as *n*-hexane. The polarity of the complexes, as expressed in terms of solubility in *n*-hexane, decreases with increasing DN. It was found that the solubility of the complexes increased with the degree of neutralization (Table 2).

Since FT-IR spectroscopy is a well established and suitable tool to analyze the proton-transfer processes,[3b] this method was applied to prove the complex formation in bulk. Due to the instability of the dry sulfonic acids **C8-H** and **C12-H**,[8] the pyridinium salts **C8-Py** and **C12-Py** had to be used as the reference material. Figure 2 presents the FT-IR spectra of **P4VP-(C12-H)$_{DN}$** compounds together with that of the model compound **C12-Py** and the pure P4VP. Similar to the literature,[3b] the stretching mode band at of the pyridine ring 993 cm^{-1} of the pure P4VP completely disappeared at full protonation. This band is replaced by two others of similar intensity situated at 1007 and 1030 cm^{-1}. Figure 2b demonstrates the appearance of a strong band at 1636 cm^{-1} in the complex samples. The 1597 cm^{-1} band (stretching mode of the pyridine ring) of P4VP is replaced by a 1585 cm^{-1} band of the benzene ring from **C12-H**. This is a qualitative evidence of the formation of pyridinium ions from the pyridine groups. The small band at 1674 cm^{-1}, which corresponds to traces of DMF, completely disappeared even at the very low degree of neutralization (Figure 2b). Thus, FT-IR analysis demonstrated that in bulk material the equilibrium between P4VP and **C12-H** was shifted completely toward ionized species.

The phase behavior of the complexes was also studied by means of POM, DSC, and X-ray diffraction. The obtained results are summarized in Table 3.

According to POM data, all complexes studied here, including the one with the lowest degree of neutralization (DN = 0.13), show birefringent textures from room temperature until isotropization. Complexes **P4VP(C12-H)$_{DN}$** with low degrees of neutralization (DN ≤ 0.50) and all complexes **P4VP(C8-H)$_{DN}$** display similar strongly birefringent textures (Figure 3a), while textures of low birefringence were observed for complexes **P4VP(C12-H)$_{DN}$** with a degree of neutralization above 0.80 (Figure 3b).

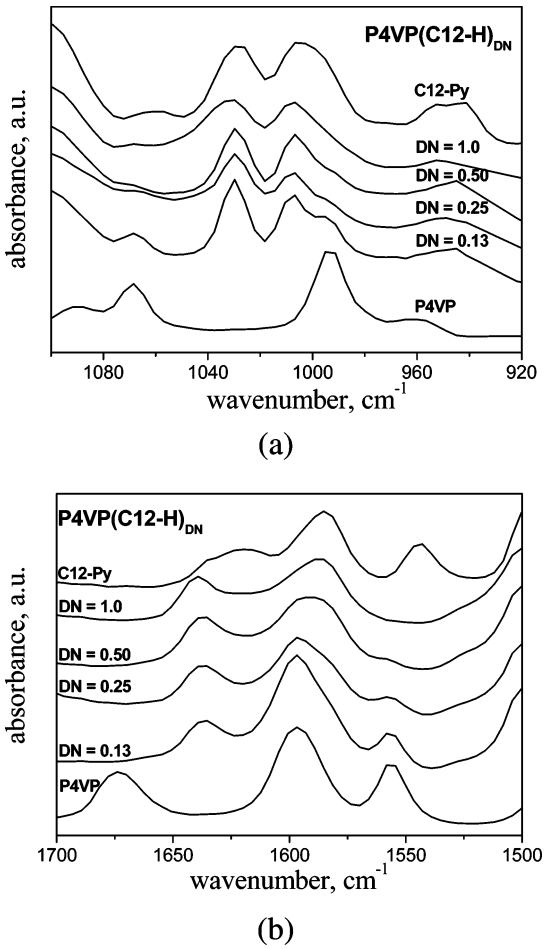

Figure 2. Infrared spectra recorded in the 920−1100 cm^{-1} (a) and 1500−1700 cm^{-1} (b) regions obtained from **P4VP(C12-H)$_{DN}$** (DN = 0.13, 0.25, 0.50, 1.0), P4VP, and **C12-Py**.

Table 3. Phase Behavior of Complexes **P4VP(C12-H)$_{DN}$** and **P4VP(C8-H)$_{DN}$**

complex	mesophase	T_{iso},[a] °C	T_g,[b] °C
P4VP(C8-H)$_{0.25}$	Lam	250	137
P4VP(C8-H)$_{0.50}$	Lam	275	143
P4VP(C8-H)$_{1.0}$	Col$_{hd}$	209	not detected
P4VP(C12-H)$_{0.13}$	Lam	225	137
P4VP(C12-H)$_{0.25}$	Lam	250	136
P4VP(C12-H)$_{0.33}$	Lam	253	139
P4VP(C12-H)$_{0.50}$	Lam	260	148
P4VP(C12-H)$_{0.80}$	Col$_{hd}$	190	not detected
P4VP(C12-H)$_{1.0}$	Col$_{hd}$	190	not detected

[a] T_{iso} = isotropization temperature measured by POM. [b] T_g = glass transition temperature measured by DSC.

Because of the slow formation of the mesophase on cooling from the isotropic phase and an observed decomposition process near the complex melting temperatures, a special procedure was used to measure the DSC thermograms. Because of the decomposition accompanying the isotropization process, the thermal history cannot be removed by annealing in the isotropic state. To generate a reproducible reference state, the samples

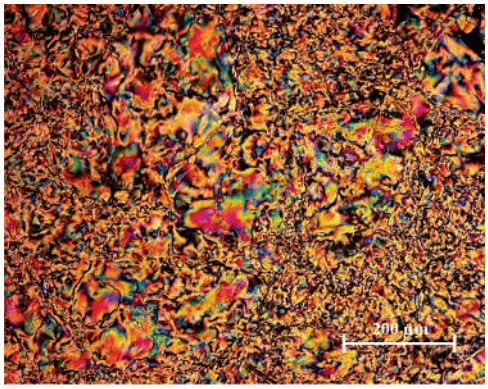

(a)

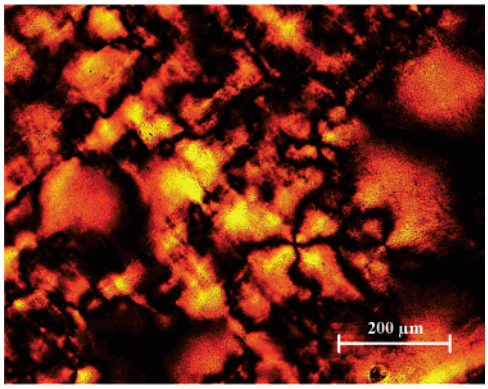

(b)

Figure 3. Polarizing optical micrographs of complexes **P4VP(C12-H)$_{0.5}$** (a) and **P4VP(C12-H)$_{1.0}$** (b) at 200 and 150 °C, respectively.

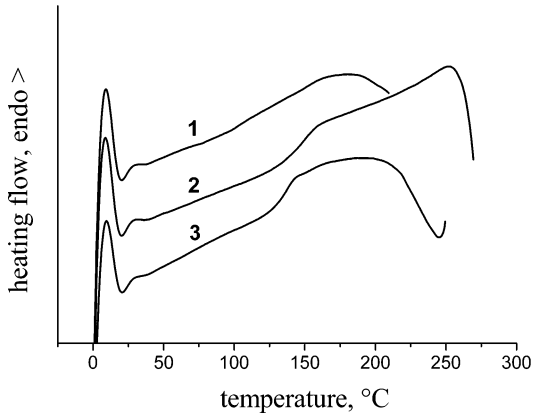

Figure 4. Representative DSC traces of the complexes recorded during the second heating run: 1, **P4VP(C12-H)$_{0.80}$**; 2, **P4VP(C12-H)$_{0.50}$**; 3, **P4VP-(C12-H)$_{0.13}$**. The heating rate was 10 K min^{-1}.

were first heated to 160 °C and subsequently cooled to 0 °C. The second heating was carried out from 0 °C to a temperature 20 °C above the isotropization temperature of the complexes determined previously by POM. No peaks corresponding to the isotropization of the complexes were observed; in the region of the clearing point a strong exothermal process occurred (Figure 4). This observation is quite similar to the DSC traces recorded for the P4VP complexes with 1,3-propanedisulfonic acid;[13] however, the authors did not give any explanations. We assume that the exotherm might be caused by an exothermal

(13) Shibata, M.; Kimura, Y.; Yaginuma, D. *Polymer* **2004**, *45*, 7571−7577.

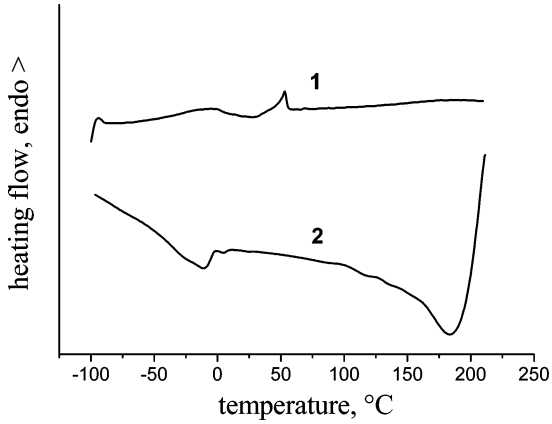

Figure 5. DSC heating trace (10 K min^{-1}) of the complex **P4VP(C12-H)$_{0.80}$** (curve 1) subsequent to quenching from 210 °C at 40 K min^{-1} (curve 2).

reaction initiated by the melting of the complexes. According to thermal gravimetric analysis (TGA), all the complexes start to lose weight at about 270 °C, which is higher than the onset temperature of the exothermic reaction. It should be noted that this exothermic reaction is much less pronounced in the case of higher DN values (DN ≥ 0.80).

Glass transitions can clearly be seen in the DSC curves for the complexes with DN ≤ 0.50 (Figure 4). Under the same measurement conditions the complexes with DN ≥ 0.80 did not display any vitrification process. However, by quenching of the isotropic melt, an endothermal peak appeared on the DSC traces of the amorphous samples of **P4VP(C12-H)$_{0.80}$** and **P4VP(C12-H)$_{1.0}$** at about 50 °C (Figure 5). At this temperature the complexes soften; hence, it might be due to the "defreezing" of the side groups. Glass transition was also not detected for the **P4VP(C8-H)$_{1.0}$** complex, and no visible transitions appeared on the DSC curve of the quenched sample.

X-ray diffraction measurements were used to identify the types of mesophases formed by these complexes. Figure 6a presents a 2D X-ray pattern of an oriented fiber of **P4VP(C12-H)$_{0.50}$** complex at 25 °C. In the SAXS region, a set of two equatorial reflections with *s*-spacings given by the ratio 1:2 were observed. These reflections can be indexed as the 001 and 002 reflections of a lamellar phase. The wide-angle pattern (not shown here) does not reveal any other features indicating that the studied compound is in a liquid crystalline state. According to the X-ray experiments, all complexes **P4VP(C12-H)$_{DN}$** with lower degree of neutralization (DN ≤ 0.50) form lamellar phases.

By contrast, the **P4VP(C12-H)$_{DN}$** complexes with higher degrees of neutralization (DN ≥ 0.80) form a Col$_{hd}$ phase. 1D X-ray patterns recorded for complexes **P4VP(C12-H)$_{0.80}$** and **P4VP(C12-H)$_{1.0}$** at 25 °C are given in Figure 7. In the SAXS region, the **P4VP(C12-H)$_{0.80}$** complex exhibit three peaks located at s = 0.012, 0.020, and 0.249 Å^{-1} (Figure 7a). The ratio of the measured *s*-spacings was found to be 1:$\sqrt{3}$:2; therefore, these reflections can be attributed to 10, 11, and 20 reflections of a hexagonal columnar lattice with a lattice parameter of 96.9 Å. For the complex with fully neutralized pyridine unites **P4VP(C12-H)$_{1.0}$** only two reflections with the *s*-spacing given by the ratio 1:$\sqrt{3}$ were recorded in the SAXS region that can also be indexed to 10 and 11 reflections of a Col$_{hd}$ phase.

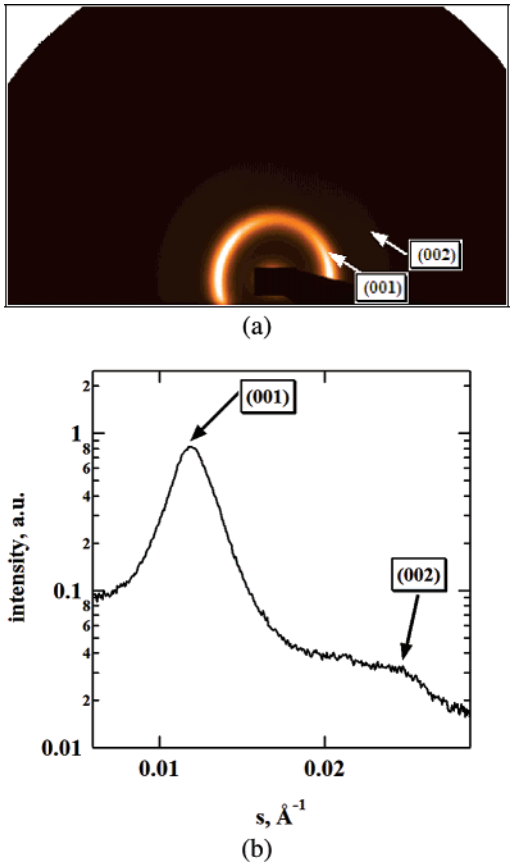

Figure 6. 2D X-ray diffraction pattern (a) and the corresponding 1D diffractogram (b) of **P4VP(C12-H)$_{0.50}$** complex recorded at 25 °C. The fiber axis is vertical.

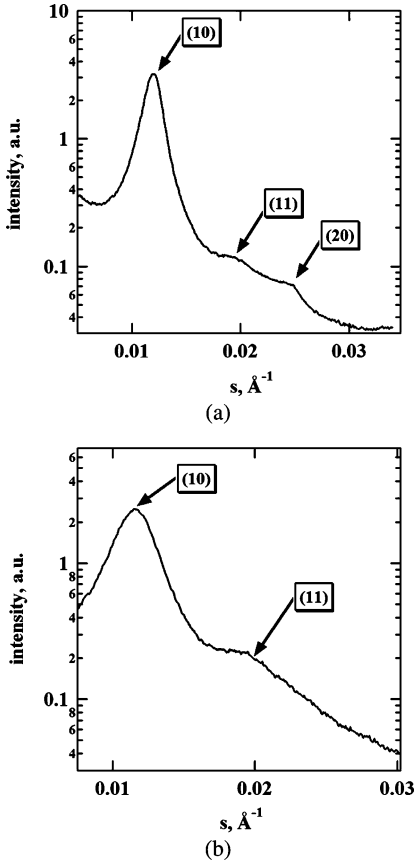

Figure 7. 1D X-ray diffraction patterns of **P4VP(C12-H)$_{0.80}$** (a) and **P4VP-(C12-H)$_{1.0}$** (b) complexes recorded at 25 °C.

The interlayer distances (d_{10}, d_{001}) as well as the corresponding lattice parameters (a, c) of the complexes measured at 25 °C are summarized in Table 4. For complexes forming a lamellar phase, the interlayer distance (d_{001}) decreases with DN, which can be explained by the thinning of the P4VP layer. Similar behavior was observed previously for the side-chain liquid crystalline polymers by dilution of the mesogenic moiety.[14] This can be explained by chain stretching or a decrease of the number of P4VP polymer chains per smectic layer with increasing DN. The length of a **C12-H** molecule was estimated to be 3.1 nm from space-filling models (assuming stretched alkyl chains). By comparing this value to the lattice parameters of the mesophases formed by the **C12-Na** compound, one can assume a bilayer type of packing. Considering the diameter of one P4VP chain being around 0.9 nm, it seems that there is no interpenetration of the side groups in these complexes. A schematic representation of the proposed packing model for **P4VP(C12-H)$_{DN}$** (DN $\leq$ 0.50) is illustrated in Figure 8a. The side groups and the P4VP polymer backbones form alternating layers, and in the polymer layers the P4VP chains are not distinguishable.

Similarly to block-copolymers, an increase in the volume fraction of one of the phases induces a spontaneous interfacial curvature that destabilizes the lamellar morphology[15,16] and eventually leads to a localization of the undulation. Thus, when a DN of 80% is exceeded, a Col$_{hd}$ phase is formed (Figure 8b). The P4VP backbones become isolated from each other by the side wedge-shaped groups. Interestingly, a considerable increase of the lattice parameter can be observed with respect to the complexes with lower DN. For instance, when DN changes from 0.50 to 0.80, the lattice parameter increases for about 30%. This behavior indicates a conformational change of the P4VP backbone during the transition from lamellar to columnar mesophase. Considering that the densities of the two phases are similar, the increase of the lattice parameter should be accompanied by a decrease of the contour length of the polymer backbone. The reduced length of the chain was previously attributed to a disordered helixlike conformation.[6] Further increase of DN from 80% to 100% causes a slight thickening of the supramolecular cylinders.

The **P4VP(C8-H)$_{DN}$** complexes exhibit a similar phase behavior. Figure 9 shows 1D X-ray patterns of these samples annealed for 5 min at 160 °C. A more clear dependence of the

Table 4. Interlayer Distances d_{001} of the Lamellar Phase and d_{10} of the Col$_{hd}$ Phase as Well as the Corresponding Lattice Parameters c and a of Complexes **P4VP(C12-H)$_{DN}$** and **P4VP(C8-H)$_{DN}$** at 25 °C

complex	mesophase	d_{001}, c, Å	d_{10}, Å	a, Å
P4VP(C12-H)$_{0.13}$	Lam	80.0		
P4VP(C12-H)$_{0.25}$	Lam	78.0		
P4VP(C12-H)$_{0.50}$	Lam	73.5		
P4VP(C12-H)$_{0.80}$	Col$_{hd}$		83.9	96.9
P4VP(C12-H)$_{1.0}$	Col$_{hd}$		86.8	100.2
P4VP(C8-H)$_{0.25}$	Lam	67.5		
P4VP(C8-H)$_{0.50}$	Lam	59.2		
P4VP(C8-H)$_{1.0}$	Col$_{hd}$		60.8	70.2

(14) Diele, S.; Oelsner, S.; Kuschel, F.; Hisgen, B.; Ringsdorf, H. *Mol. Cryst. Liq. Cryst.* **1988**, *155* (Pt. B), 399−408.
(15) Bates, F. S.; Fredrickson, G. H. *Annu. Rev. Phys. Chem.* **1990**, *41*, 525−557.
(16) Hamley, I. W. *The Physics of Block Copolymers*; Oxford, U.K., New York, 1998.

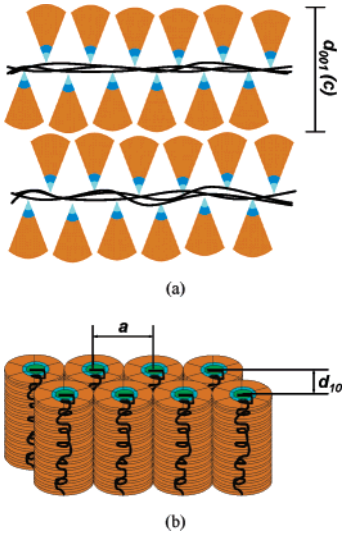

Figure 8. Proposed packing model of complexes **P4VP(C12-H)$_{DN}$** in the lamellar phase (DN ≤ 0.50) (a) and in the hexagonal columnar phase (DN ≥ 0.80) (b).

phase structure on DN can be seen. Complex **P4VP(C8-H)$_{0.25}$** shows a typical X-ray pattern of a lamellar phase, while complex **P4VP(C8-H)$_{1.0}$** forms a Col$_{hd}$ phase. By contrast, only a broad reflection peak is observed for the complex with intermediate DN value—**P4VP(C8-H)$_{0.5}$**. This might be caused by a spontaneous curvature of the smectic layers,[2a] which results in the formation of a modulated smectic phase. In the case of **P4VP-(C8-H)$_{DN}$** interplanar distances (Table 4) depend on the DN in a similar manner as for **P4VP(C12-H)$_{DN}$**, i.e. first decreasing and then increasing. However, the variation in this case is much less significant.

The temperature behavior of the lamellar as well as the columnar phases formed by the **P4VP(C12-H)$_{DN}$** complexes was investigated by temperature-dependent X-ray diffraction. For all the complexes a remarkable decrease of the characteristic distance was observed on heating starting from 50 to 60 °C (Figure 10). In this temperature range, the DSC curves of the complexes with higher DN values reveal an endothermal peak. Therefore, one can speculate that this temperature corresponds to "defreezing" of the side groups. Such thermal behavior of the interlayer distance was observed earlier for columnar mesophases formed by monodendron-jacketed polymers.[17]

Figure 11 shows the phase diagram of the complexes **P4VP-(C12-H)$_{DN}$** summarizing the POM, DSC, and X-ray data. The complex with DN = 0.50 shows the highest isotropization temperature. Isotropization temperature increases with increase of DN until 0.50 due to the enlargement of liquid crystalline domains. At the transition from lamellar to columnar mesophase, the isotropization temperature falls down drastically. At lower DN values due to the lamellae formation of the strong-microphase separated systems, the glass transition of the complexes is mainly governed by the P4VP backbones; the sulfonic acid side groups have a minor influence on it. When it exceeds a DN of 0.80, the complex molecule starts to behave as an individual supramacromolecule; thus, these materials do not show any significant glass transition in the temperature range from −100 °C to isotropization. The dissolution process of the

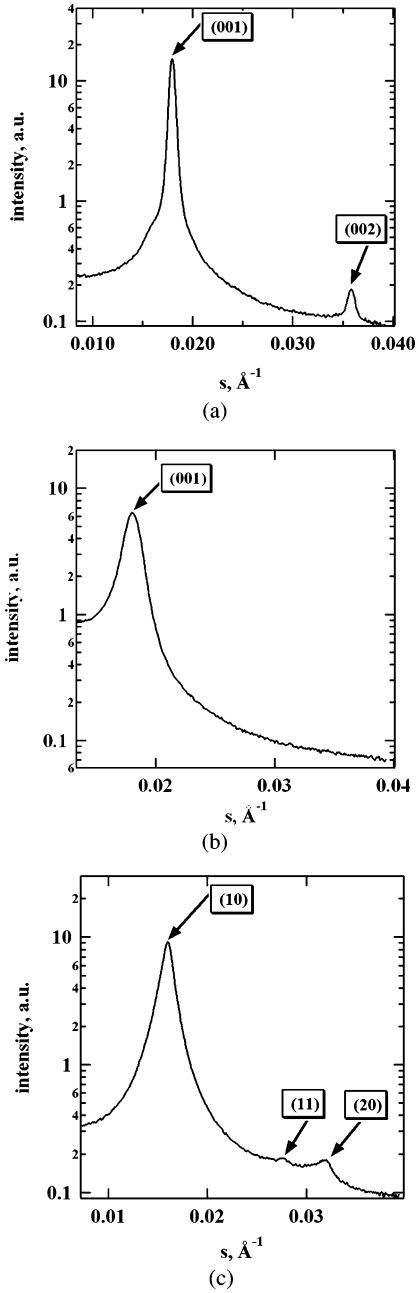

Figure 9. X-ray diffraction patterns of complexes **P4VP(C8-H)$_{0.25}$** (a), **P4VP(C8-H)$_{0.50}$** (b), and **P4VP(C8-H)$_{1.0}$** (c). Before measurements at 25 °C, the samples were annealed for 5 min at 160 °C.

complexes with higher DN values is much faster than that of the others; this is an indication of an efficient plasticizing. Complexes **P4VP(C8-H)$_{DN}$** showed a similar trend (Table 3); however, their isotropization temperatures were found to exceed that of the C12 derivates.

Since the ligand molecules contain an azo-chromophore, UV−vis spectroscopy can be used to follow the self-assembling process by monitoring the changes of the optical absorption properties.[18]

The UV−vis spectra were recorded from dilute solutions in chloroform. Figure 12 shows the UV−vis spectra of **P4VP-**

(17) Chvalun, S. N.; Shcherbina, M. A.; Bykova, I. V.; Blackwell, J.; Percec, V.; Kwon, Y. K.; Cho, J. D. *Polym. Sci., Ser. A* **2001**, *43*, 33−43.

(18) (a) Song, X.; Perlstein, J.; Whitten, D. G. *J. Am. Chem. Soc.* **1997**, *119*, 9144−9159. (b) Buwalda, R. T.; Stuart, M. C. A.; Engberts, J. B. F. N. *Langmuir* **2002**, *18*, 6507−6512. (c) Priimagi, A.; Cattaneo, S.; Ras, R. H. A.; Valkama, S.; Ikkala, O.; Kauranen, M. *Chem. Mater.* **2005**, *17*, 5798−5802.

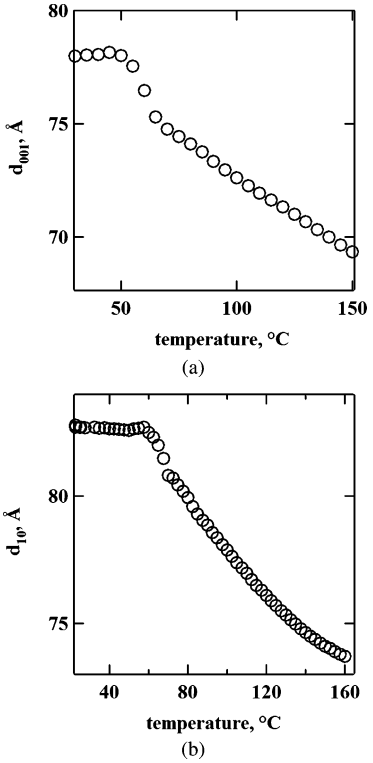

Figure 10. Temperature variation on heating of the interlayer distance d_{001} for the complex **P4VP(C12-H)$_{0.25}$** (a) and d_{10} for **P4VP(C12-H)$_{0.80}$** (b).

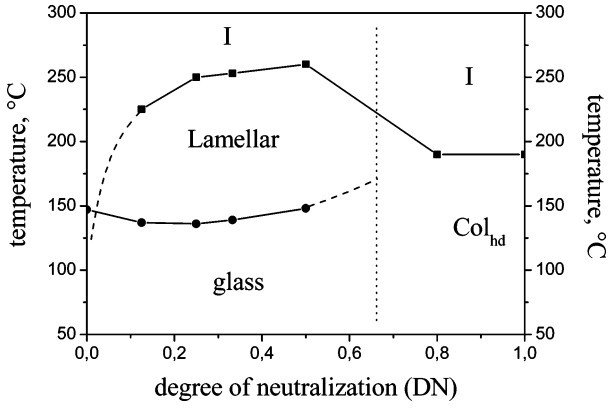

Figure 11. Phase diagram of complexes **P4VP(C12-H)$_{DN}$**.

(C12-H)$_{DN}$ complexes with different DN values. The spectra are similar, consisting of a large band with a maximum in the area of 330 nm, corresponding to the $\pi-\pi^*$ transition of the azo-chromophore. The double band with maxima at approximately 255 and 263 nm corresponds to the $\pi-\pi^*$ transitions of benzene and pyridine rings, respectively, while the broad weak band in the area of 450 nm corresponds to the $n-\pi^*$ transition of the azo-group. On increase of the degree of neutralization, the wavelength of the absorption maximum λ_{max} of the azo-group $\pi-\pi^*$ bands shifts to smaller values (blue shift, cf. Figure 13). Figure 13 depicts a plot of λ_{max} versus the degree of neutralization for both series of complexes. The absorption wavelength decreases monotonically from 332 nm (**P4VP(C12-H)$_{0.13}$**) to 324 nm (**P4VP(C12-H)$_{1.0}$**), and the slope of the λ_{max}/DN curve becomes smaller with growing DN ($[d\lambda_{max}/d(DN)]_{DN=0.12} = -28.8$ nm, $[d\lambda_{max}/d(DN)]_{DN=1} = -1.1$ nm). The **P4VP(C8-H)$_{DN}$** complexes exhibit very similar spectral properties; however, their absorption maxima are always red-shifted

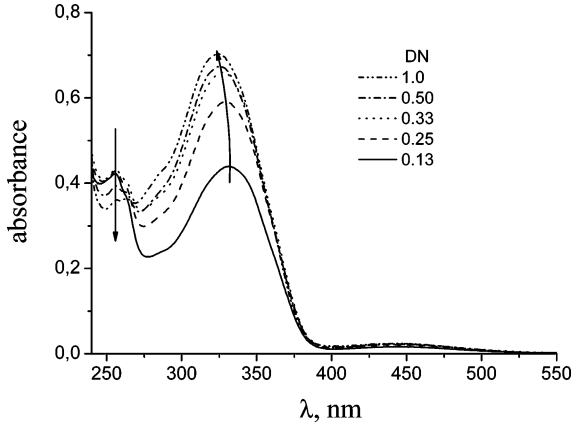

Figure 12. UV−vis spectra of complexes **P4VP(C12-H)$_{DN}$** at different DN values (solvent = chloroform; concentration = 0.03 mg/mL).

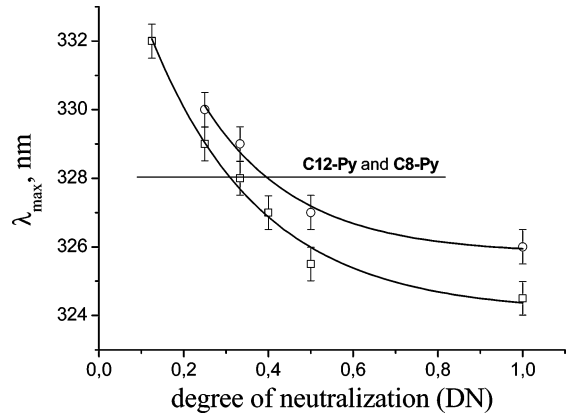

Figure 13. Absorption maximum wavelength of the azo-groups $\pi-\pi^*$ band, λ_{max}, of the complexes **P4VP(C12-H)$_{DN}$** (□) and **P4VP(C8-H)$_{DN}$** (○) versus the degree of neutralization (DN).

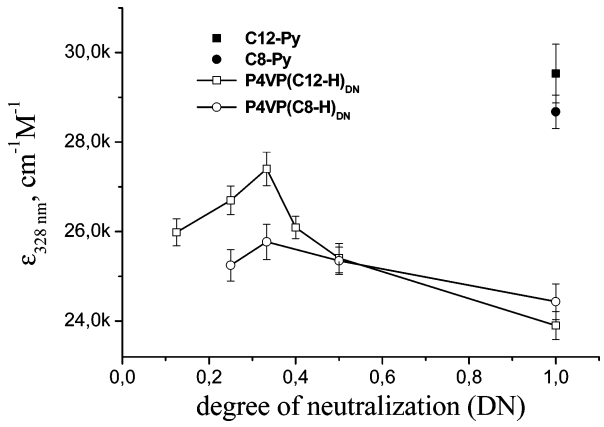

Figure 14. Plot of molar extinction coefficient of the azo-chromophores at 328 nm (ϵ_{328}) versus the degree of neutralization.

by about 1 nm with respect to that of the **P4VP(C12-H)$_{DN}$** complexes. In Figure 13 the wavelength of the respective absorption maximum of both the model compounds **C8-Py** and **C12-Py** (λ_{max} = 328 nm) is marked. The wavelength of the complexes becomes identical with the wavelength of the model compounds at degrees of neutralization between $DN_{id} \approx 0.30$ (**P4VP(C12-H)$_{0.30}$**) and $DN_{id} \approx 0.40$ (**P4VP(C8-H)$_{0.40}$**).

Figure 14 depicts a plot of the molar absorption coefficient at 328 nm (ϵ_{328}) of both series of macromolecular complexes as a function of the degree of neutralization. The azo-chromophores in the complexes exhibit lower molar absorp-

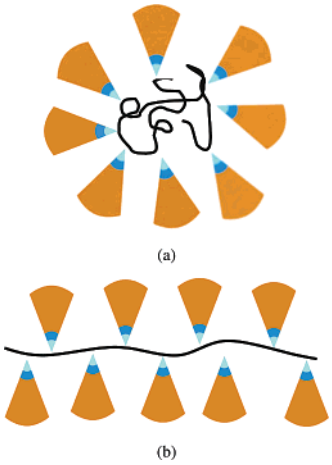

Figure 15. Schematic depiction of the complex structures at low DN (<0.33) (a, "ligand surrounded random coil") and at high degree of substitution (DN > 0.33; b, "jacketed macromolecule").

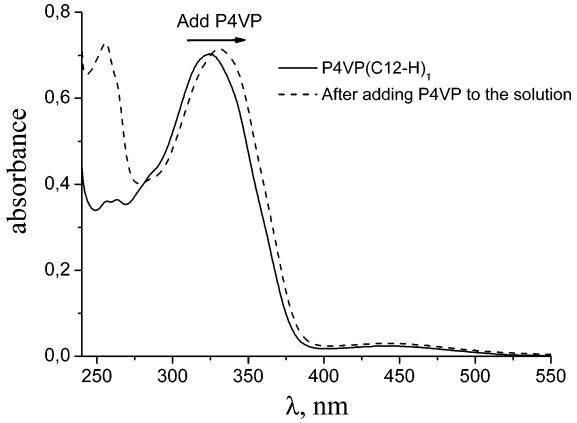

Figure 16. Change of the UV−vis spectra of **P4VP(C12-H)$_{1.0}$** to **P4VP-(C12-H)$_{0.13}$** by adding a corresponding amount of P4VP to its chloroform solution. The molar concentration of the sulfonic acid is 0.0285 mmol/L.

tivities than that of the pyridinium salt model compounds; i.e., a hypochromic effect is present. On comparison of the ϵ_{328} values of the model compounds to that of the fully neutralized complexes, a hypochromic value of 19% was measured for the pair **P4VP(C12-H)$_{1.0}$/C12-Py**, while a value of 15% was found for **P4VP-(C8-H)$_{1.0}$/C8-Py**.

The molar absorption coefficients of both complex series increase linearly from DN = 0.13 to DN = 0.33 due to the increase of effective concentration of chromophores,[19] while above DN ~ 0.33 they decrease although the chromophore concentration in the system effectively grows. With **P4VP(C12-H)$_{DN}$** complexes the maximum of the ϵ_{328}/DN curve is located around DN$_{max}$ = 0.33; this value coincides with the DN$_{id}$ values in Figure 14, where the absorption maximum wavelength of complexes and model compounds becomes identical.

The observed changes in the UV−vis spectra provide information on the molecular structures of the complexes at different degrees of complexation. Hypsochromism (blue shift) and hypochromism (decrease in molar absorptivity) are indicative for the presence of special chromophore−chromophore interactions. A blue shift of the absorption maximum can be assigned to a parallel interaction mode of the chromophores, the so-called H-aggregation.[20] Hypochromism is a powerful indicator on the relative orientation of chromophores as commonly observed in DNA, RNA, and other polymers.[21,22] It is also well-known that hypochromic effects are sensitive to the distance between chromophores by r^{-3}.[21]

Note that Beer's law was obeyed for all the complexes with concentrations less than 0.08 mg/mL. Thus, both observed effects demonstrate that ligands become bound to the P4VP backbone on the time scale of electronic transitions and that at high DN values the bound ligands interact more strongly than the molecularly dissolved model compounds at the same concentration. For chromophores that are bound to a macromolecule such a behavior is justified, since the local concentration of chromophores in such a complex is large; i.e., the distance between the units become small. The macromolecular chain holds the chromophores units close to each other and increases their interaction; consequently the hypochromic effect should arise predominantly from intramolecular interactions between the side groups. The maximum of the absorptivity/degree of neutralization curve at DN$_{max}$ = 0.33 indicates a distinct change of the interchromophore interaction below and above this limit that can only be caused by a local transition in relative orientation of the chromophores within the supramolecules. Since the ligand molecules are connected to the polymer backbone via ionic attractions, their arrangement cannot be independent of the chain conformation.

It has to be concluded that at a degree of substitution of DN ≈ 0.33 a transition of the polymer chain from a statistical coil in another, most probably stretched and more ordered, conformation occurs (Figure 15). It was observed that the hypochromic effect was more pronounced in the case of **P4VP(C12-H)$_{DN}$** than for **P4VP(C8-H)$_{DN}$** complexes. **C12-H** ligand molecules are more space demanding than the **C8-H** units, and for this reason the conformational transition should occur at somewhat larger degree of substitution as it is indicated by the data in Figures 13 and 14.

Figure 16 shows the result of a further experiment, where first the spectrum of the complex **P4VP(C12-H)$_{1.0}$** was recorded (full line). To this solution pure poly(4-vinylpyridine) was added; the polymer amount was sufficiently large to change the total composition of the system from **P4VP**:**C12-H** = 1:1 to a value of 1:0.13. Subsequently, the spectrum of the mixture was measured (dotted line), which was found to be identical with the spectrum of the complex **P4VP(C12-H)$_{0.13}$** as depicted in Figure 12. Obviously, the ligand molecules **C12-H** redistributed along all present polybase chains. The complex **P4VP-(C12-H)$_{1.0}$** disintegrated and became replaced by complexes **P4VP(C12-H)$_{0.13}$**. Therefore, it can be concluded that the ligand molecules are not permanently fixed at a given polybase chain; instead a dynamic exchange equilibrium must exist, similar to the exchange equilibrium known from surfactant micelles.[23] It is clear that under such circumstances the addition of noncomplexed polybase chains drives the distribution of the ligand molecules toward equidistribution, i.e., identical degree of protonation for all polymer chains in full accordance with le Chatelier's principle.

(19) Nelson, J. C.; Saven, J. G.; Moore, J. S.; Wolynes, P. G. *Science* **1997**, *277*, 1793−1796.
(20) McRae, E. G.; Kasha, M. *J. Chem. Phys.* **1958**, *28*, 721−722.
(21) Bloomfield, V. A.; Crothers, D. M.; Tinoco, I. *Physical Chemistry of Nucleic Acids*; Harper & Row: New York, 1974.
(22) Cantor, C. R.; Schimmel, P. R. *Biophysical Chemistry*; Freeman: New York, 1980.

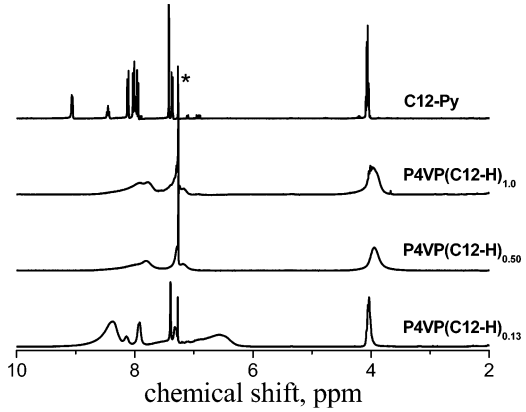

Figure 17. ^{1}H NMR spectra of complexes **P4VP(C12-H)$_{DN}$** and monomeric analog **C12-Py**. Spectra were normalized to the terminal methyl group. The asterisk indicates the ^{1}H signal of $CHCl_3$.

Proton nuclear magnetic resonance (^{1}H NMR) data provided additional evidence for the intramolecular interaction (Figure 17). In chloroform the ^{1}H resonance signals of model compound **C12-Py** were all sharp and well-separated, showing the expected hyperfine structure. In the complexes the signals became more broadened the closer the geometric position of a respective proton was located to the tip of the wedge. With increasing degree of neutralization, the signal broadening became more pronounced and simultaneously an upfield shift of the $-OCH_2-$ proton resonance around $\delta \sim 4$ ppm (cf. Figure 17) was observed. Obviously, the complex bound ligand molecules become less mobile and their $-OCH_2-$ protons come in close vicinity to other aromatic units, so that the ring currents of the aromates could alter the chemical shift. These results are indicative to the formation of a dense, most probably partially ordered, arrangement of the ligand molecules, as to be expected from the formation of cylindrical stacks.[24]

Conclusions

Mesogenic wedge-shaped sulfonic acid molecules were successfully linked by means of noncovalent interactions ionic to poly(4-vinylpyridine) (P4VP) chains. X-ray diffraction, polarizing optical microscopy, and differential scanning calorimetry revealed that liquid crystalline order was formed at the degree of neutralization as low as 0.13. X-ray diffraction measurements showed a transition from a lamellar to a hexagonal columnar mesophase on exceeding DN of 80%, which is at the same time accompanied by effective plasticizing, i.e., depressing of glass transition of the P4VP backbone. A drastic increase of lattice parameter at this transition probably indicates the formation of a disordered helical conformation of P4VP chains in the hexagonal columnar phase. Wedge-shaped sulfonic acid molecules bearing dodecyl chains show a higher ability to induce the columnar structure formation than amphiphilic wedges with octyl groups, while the C8 derivatives exhibit higher transition temperatures than the C12 compounds. In diluted solutions UV−vis spectroscopy showed the presence of hypsochromic as well as hypochromic effects on increasing the degree of neutralization of P4VP. The results indicate a transition of the chromophores arrangement that is bound to a transition of the polymer backbone at DN = 0.33. Most probably at this point the system transforms from "ligand-surrounded random coils" into a true cylinder-shaped complex, where the polymer chain is jacketed by the wedge shaped ligands. No information on the conformation of the polymer chain within these cylinders is yet available; however, the assumption that the polymer chain is more stretched and more ordered than in a random coil seems to be justified.

Moreover, the ligands are not permanently fixed to one individual position; instead the existence of a dynamic complexation/decomplexation equilibrium was demonstrated.

In the future this approach can certainly be extended to rigid conductive polymers as polyaniline and polypyrrole. The possible formation of liquid crystalline order in such complexes is expected to open a new vista to the processing and manufacture of highly oriented conductive fibers.

Acknowledgment. The financial support of the EU (ECOPOL), AGFA, DFG (SFB 569), and Max-Buchner Stiftung is acknowledged. X.Z. thanks the Alexander von Humboldt Foundation for financial support. D.A.I. acknowledges financial support by the FNRS of Belgium, FRFC project N*o*. 2.4612.04, and the CNRS of France. R.I.G. is a postdoctoral fellow of the Centre National de la Recherche Scientifique (CNRS) of France. We acknowledge the European Synchrotron Facility for provision of synchrotron radiation facilities. We thank T. Narayanan and M. Sztucki, N. Vilayphiou, and W. Bras for assistance in using ID02 and BM26B beamlines, respectively. We are grateful to Prof. S. Rastogi for collaboration in the frame of the project on the BM26B beamline.

Supporting Information Available: The compositions and yields of the different reaction mixtures for the preparation of complexes, detailed analysis of X-ray diffraction data recorded from low molecular weight sulfonate salts, and detailed TGA and DSC measurements for complex **P4VP(C12-H)$_{0.5}$**. This material is available free of charge via the Internet at http://pubs.acs.org.

JA065968V

(23) Rosen, M. J. *Surfactant and Interfacial Phenomena*; John Wiley & Sons, Inc.: Hoboken, NJ, 2004.
(24) Rapp, A.; Schnell, I.; Sebastiani, D.; Brown, S. P.; Percec, V.; Spiess, H. W. *J. Am. Chem. Soc.* **2003**, *125*, 13284−13297.